Notes

Spectroscopic Evidence for Stereocomplex Formation by Enantiomeric Polyamides Derived from Tartaric Acid

R. Marín,[†] A. Martínez de Ilarduya,[†] P. Romero,[‡] J. R. Sarasua,[§] E. Meaurio,[§] E. Zuza,[§] and S. Muñoz-Guerra*,[†]

Departament d'Enginyeria Química, ETSEIB, Universitat Politècnica de Catalunya, 08028 Barcelona, Spain, Departamento de Química Orgánica, Instituto de Ciencia de Materiales de Aragón, CSIC-Universidad de Zaragoza, 50009 Zaragoza, Spain, and Departamento de Ciencia de Materiales, ETS de Ingeniería, Universidad del País Vasco UPV-EHU, 48013 Bilbao, Spain

Introduction

A polymer stereocomplex is formed by stereoselective coupling between two complementing stereoregular polymers. The stereocomplex characterizes by displaying altered physical properties respect to its parent polymers. Since the discovery of the first stereocomplex formed by *syn*- and *i*-PMMA in 1958,[1] a fair number of stereocomplexes, most of them consisting of pairs of complementary enantiomeric polymers, have been reported.[2] A comprehensive overview of the stereocomplexation phenomenon in both polymers and biopolymers has been recently reported by Domb.[3] Until today the use of stereocomplexes for biomedical applications has been sporadic. However, a recent series of works on the use of polylactic based stereocomplexes has evidenced the interest of these systems for controlled release and stabilization of peptide and protein drugs.[4] Stereocomplexes are looked with particular interest because of their potential as matrices for controlled drug delivery systems, tissue engineering, and other biomedical purposes.

Some years ago we reported on the stereocomplex made of enantiomeric D and L poly(hexamethylene di-*O*-methyltartaramide), abbreviated P6DMT(D) and P6DMT(L) respectively, a pair of polyamides of AA-BB type prepared from hexamethylenediamine and di-*O*-methyl D- and L-tartaric acids.[5] These are optically active polyamides showing enhanced hydrophilicity and degradability.[6] On the basis of X-ray diffraction, DSC, and ^{13}C CP-MAS NMR data, the existence of an equimolar stereocomplex, abbreviated P6DMT(D+L), melting at approximately 20 °C above its separate components was demonstrated. The crystal structure of the stereocomplex was described by a monoclinic lattice with a unit cell containing two enantiomeric

chains related by a glide plane. Computational analysis assessed the ability of the D- and L-tartaric units to cocrystallize in an energetically favored crystal structure without severe distortion of the lattice geometry. A recent study has shown that P6DMT(D+L) stereocomplex formation is very sensitive to preparation conditions and that its crystallization from the melt is delayed compared to its parent polyamides.[7] Furthermore, no stereocomplex formation was observed for other homologous polyamides P5DMT or P8DMT made from 1,5-pentanediamine and 1,8-octanediamine, indicating the extremely high structural specificity required by these polyamides to attain stable stereopair coupling.

To the best of our knowledge, P6DMT(D+L) is the only case reported so far on the formation of stereocomplexes made of nonpolypeptidic chiral polyamides. The interest of this system is therefore exceptional since it is demonstrative of the occurrence of stereocomplexation in synthetic polycondensates others than polyesters. The focus of this Note has been set on the formation of the P6DMT(D+L) stereocomplex in solution and on the influence of the history of the solution on the occurrence of the stereocomplex in the solid state coming therefrom. NMR and FTIR spectroscopies have been the techniques of choice to carry out this study. The chemical structures of P6DMT polytartaramides studied in this work are depicted in Scheme 1. They were synthesized by polycondensation in solution according to a previous report.[8] Nomenclature, molecular weight, and surface, optical and thermal properties of the two enantiomeric polyamides and the stereocomplex are given in Table 1.

The P6DMT(D+L) stereocomplex in powder form may be readily prepared by precipitation with ether from a chloroform solution containing equal amounts of the two enantiomers. On the other hand, the formation of a film of the stereocomplex by casting is a process whose efficiency is strongly affected by process conditions, specifically by solution history and evaporation rate. Figure 1a shows the evolution of the intrinsic viscosity of the 10% (w/v) chloroform solution of P6DMT(L) and the stoichiometric mixture of P6DMT(D) and P6DMT(L) at increasing standing times at room temperature. Whereas the solution of single P6DMT(L) remained unchanged, the viscosity of the mixed solution increased to reach infinite value after two days of aging. Longer times were required for gellification at lower concentrations to the point that no perceivable changes in viscosity were perceived below 2% or upon raising the tem-

Scheme 1. Chemical Structures of Polyamides Studied in This Work
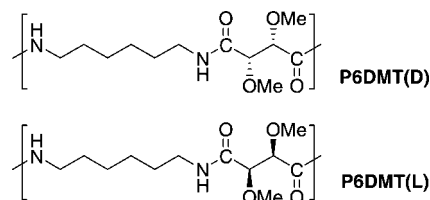
* Corresponding author. E-mail: sebastian.munoz@upc.edu.
[†] Departament d'Enginyeria Química, ETSEIB, Universitat Politècnica de Catalunya.
[‡] Departamento de Química Orgánica, Instituto de Ciencia de Materiales de Aragón, CSIC-Universidad de Zaragoza.
[§] Departamento de Ciencia de Materiales, ETS de Ingeniería, Universidad del País Vasco UPV-EHU.

Table 1. Characteristics of the Enantiomerically Pure Polyamides and Their Equimolar Mixture[a]

polyamide	η^b (dL·g⁻¹)	M_w/M_n^c (g·mol⁻¹)	contact angle (degrees)	$[\alpha]^d$ (degrees)	T_m^e (°C)	ΔH_m^e (J·g⁻¹)
P6DMT(D)	1.0	76400/36800	59.5	−92.5	232/232	52/38
P6DMT(L)	1.0	78500/37400	60.0	+90.4	233/231	54/34
P6DMT(D+L)		77950/37100	52.5	+2.0	253/251	65/56

[a] Experimental details provided as Supporting Information. [b] Intrinsic viscosity determined in dichloroacetic acid. [c] Weight and number-average molecular weights measured by GPC-LS. [d] Specific optical rotation measured in chloroform. [e] Melting temperature and enthalpy measured by DSC for the precipitated material and for the film prepared by casting from chloroform.
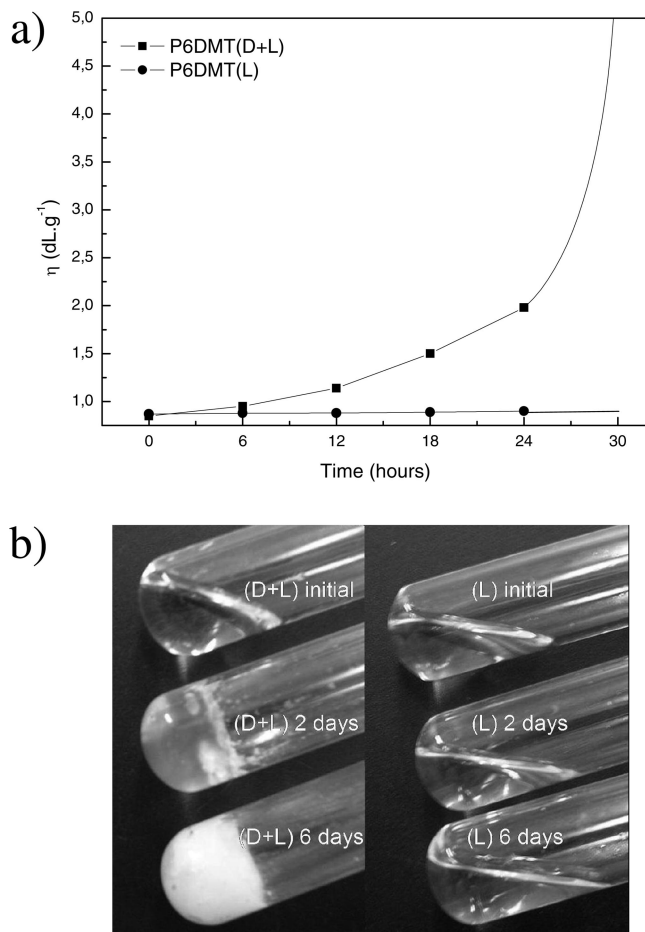

Figure 1. Evolution of the intrinsic viscosity of P6DMT(D+L) and P6DMT(L) 10% chloroform solutions with time (a) and photographs of these solutions aged at room temperature for the labeled time periods (b).

perature. Visual changes taking place in the 10% chloroform solution with time at room temperature are shown in Figure 1b; whereas the appearance of the P6DMT(L) solution did not change, the P6DMT(D+L) solution turned into a transparent gel after 24 h and ended as a white precipitate after 48 h of aging. This visually comparative experiment revealed the time dependent sol–gel transformation taking place in the mixed enantiomeric solution concomitant to the formation of the stereocomplex. A similar observation has been reported for a triblock copolymer containing segments of D- and L-polylactic acid, which interlock in aqueous solution to form a temperature-dependent stereocomplex.[9]

The stereocomplexation process happening in solution was followed by ¹H NMR. The unidimensional spectra recorded at increasing times from 5% (w/v) chloroform solutions of P6DMT(L) and P6DMT(D+L) are shown in Figure 2. Significant differences concerning the signals profile are observed between the two sets of spectra. Whereas no changes could be perceived in the spectra of the solution of the pure enantiomer, a noticeable peak broadening was observed in the spectra of the mixture

after 3 days of standing. This observation is a clear indication of an increasing restriction in the molecular mobility of the polyamide chains, which should be reasonably interpreted as due to the stereoselective coupling taking place between the two enantiomorphs. Since the broadening effect affects to all the peaks contained in the spectra it can be inferred that both main chain and side chain groups are restricted in mobility although only the latter are expected to be involved directly in the interlocking mechanism leading to the formation of the stereocomplex.

Additional evidence on the stereoselective interaction taking place in the enantiomeric pair in chloroform solution was provided by bidimensional ¹H NMR diffusion ordered spectroscopy (DOSY).[10] The DOSY spectra of P6DMT(D), P6DMT(L) and P6DMT(D+L) are comparatively displayed in Figure 3. As expected, peak broadening in the spectra of the mixture compared to the spectra of the pure enantiomorphs was apparent. To have a quantitative insight into the change in molecular mobility taking place in the solute upon mixing, the diffusion coefficients of each enantiomorph were estimated when separately dissolved and when dissolved together in stoichiometric amounts. Diffusion coefficients D were calculated by defining a reduced diffusion coefficient as the ratio of the diffusion coefficient of the enantiomorph to that of TMS in the sample.[11] D values resulting from such analysis were 3.57×10^{-11} and 3.67×10^{-11} m²·s⁻¹ for P6DMT(D) and P6DMT(L), respectively and 2.22×10^{-11} m²·s⁻¹ for the components of the P6DMT(D+L) mixture. The diffusion coefficient of TMS in the solution containing the single enantiomorphs was 1.80×10^{-9} and 1.68×10^{-9} in the solution containing the D+L mixture. The reduced diffusion coefficients were therefore $D^D/D^{TMS} = 202$, $D^L/D^{TMS} = 196$ and $D^{D+L}/D^{TMS} = 130$, indicating a decrement close to 33% for the mixture.

Diffusivity is affected by both molecular size and shape as well as by intermolecular interactions operating in solution. The equation of Stokes–Einstein relates the diffusion coefficient with the hydrodynamic radius. For small molecules it is known that a doubling in the molecular weight result in a decrease in D of 26% or 18% for spherical and elongated molecules, respectively. Unfortunately, this relationship is not so clear in polymeric samples.[12] A detailed account of the calculations including the plots leading to graphical evaluation of D is provided in the Supporting Information.

In order to asses how the solution history may determine the presence of the complex in the solid left after evaporation, this was analyzed by DSC. As it is seen in Figure 4, melting of the solid coming from the gellified mixture of P6DMT(D) and P6DMT(L) in chloroform took place 20 °C above the melting temperature of the film coming from the single P6DMT(L) solution. According to previous works,[5,7] such an increment in the melting temperature is taken as demonstrative of the presence of stereocomplex. On the contrary, the film prepared from the fresh solution of the enantiomeric mixture did not show any increment in the melting temperature, indicating that the stereocomplex was not formed in this case. These results indicate that the presence of stereocomplex in the solid prepared by
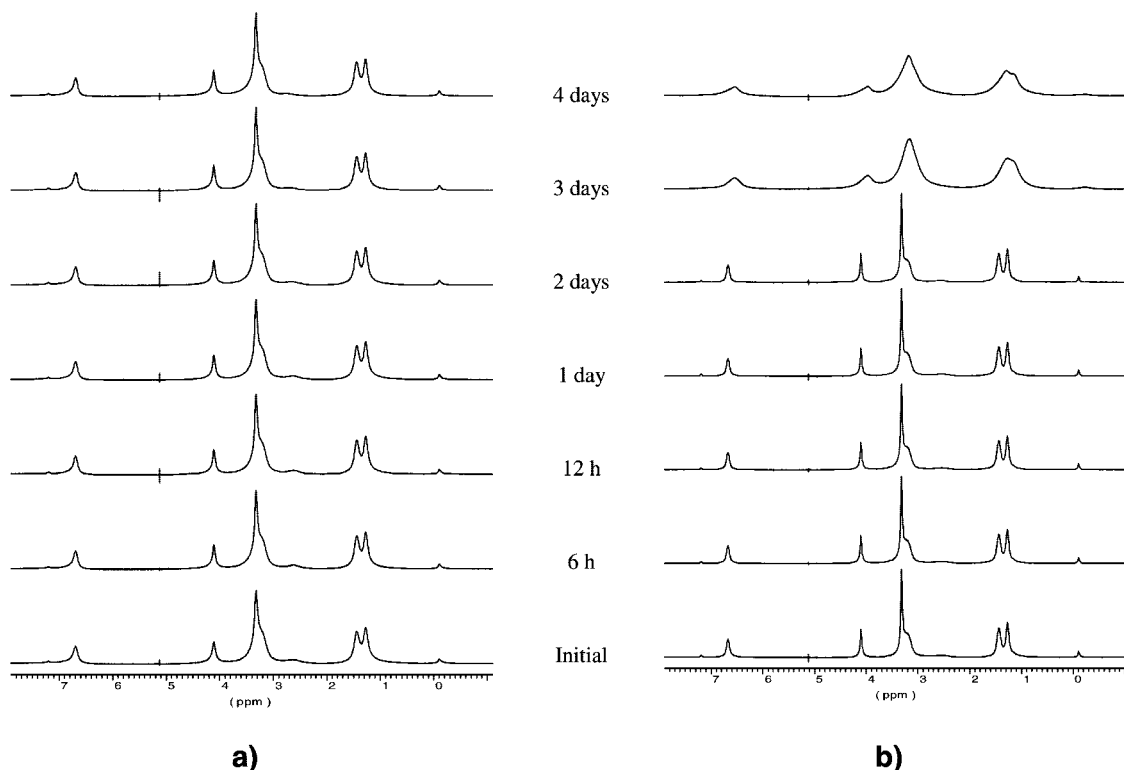
Figure 2. Evolution of the ^{1}H NMR spectra of P6DMT(L) (a) and P6DMT(D+L) (b) chloroform solutions with time at the indicated intervals.
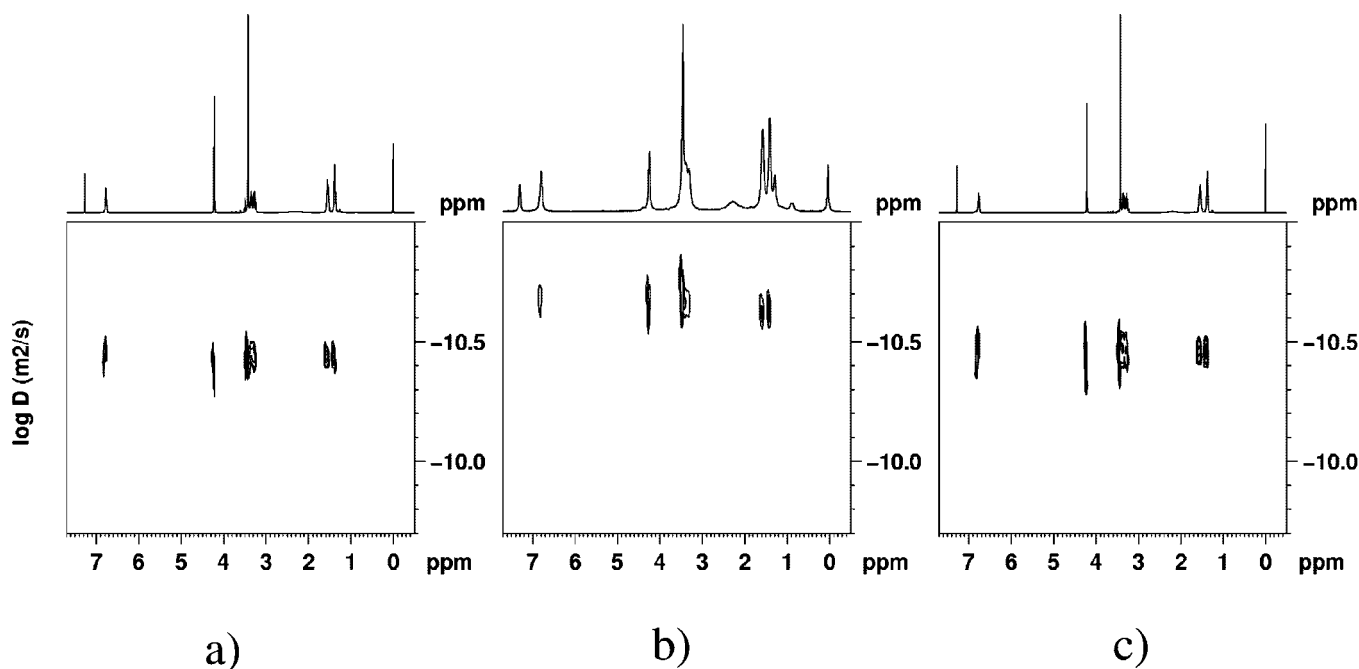

Figure 3. DOSY spectra of P6DMT(L) (a), the P6DMT(D+L) mixture (b), and P6DMT(D) (c).

evaporation requires previous stereocoupling between the two enantiomorphs in the mother solution.

The occurrence of the stereocomplex in the mixed film was proved by FTIR analysis, which also provided valuable information on the nature of the intermolecular interactions that govern the stereocomplex formation. Samples for this study were prepared by solvent evaporation of the chloroform solution and subsequently subjected to heating at 160 °C for 1 h in order to promote crystallization of those being initially amorphous. The most characteristic spectral regions of P6DMT polytartaramides

are shown in Figure 5, where traces for the P6DMT(L) sample before and after the heating treatment and for the heated P6DMT(D+L) sample are closely compared. A broad profile indicative of amorphous state is displayed by the amide I band (Figure 5a) in the spectrum of non-heat-treated P6DMT(L). The second derivative curve of this band revealed the presence of two components at 1678 and 1656 cm^{-1} attributable to free and hydrogen-bond associated carbonyl groups, respectively. After the heating treatment, this band appears narrower and shifted slightly to lower wavenumbers. Such changes reflect the
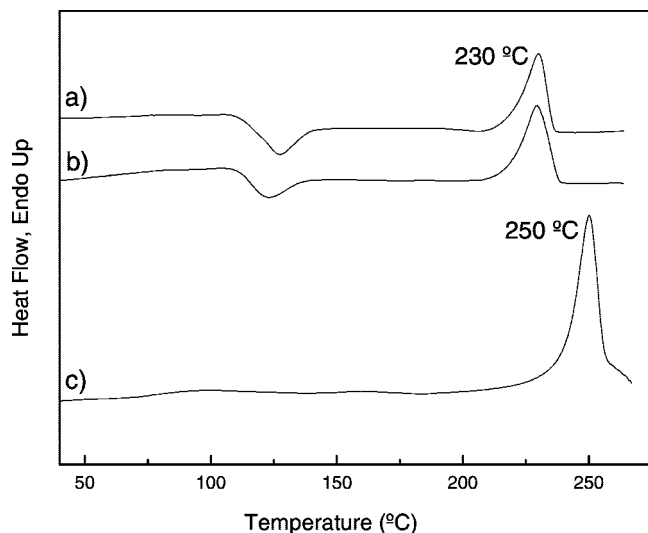
Figure 4. DSC traces of films from chloroform solution of P6DMT(L) (a), fresh P6DMT(D+L) mixture (b), and gellified P6DMT(D+L) mixture (c).

contribution of a third component located at 1654 cm^{-1}, which arises from hydrogen bonded carbonyl groups located in the crystalline domains. The amide I band of P6DMT(D+L) displayed features identical to those for crystallized P6DMT(L), suggesting a similar hydrogen bonding strength in the two systems. Similar results were obtained in the analysis of the NH stretching band. These results are in full agreement with the DSC observation described above and depicted in Figure 4, which revealed that the film made of single L-enantiomer was amorphous and crystallized upon heating whereas the material obtained from the gellified P6DMT(D+L) mixture was initially crystalline.

In the fingerprint region of these spectra, the band at 1096 cm^{-1} (Figure 5b) of these polytartaramides corresponding to the C−O−C asymmetric stretching is prominent. The most noticeable change affecting this band is the decrease of intensity observed in the case of the stereocomplex spectrum. Such a decrease is related to the lower transition moment displayed by this group in the crystalline structure of the stereocomplex compared to P6DMT(L). This leads us to conclude that the OCH$_3$ side groups must display different orientations in the crystal structures of P6DMT(L) and P6DMT(D+L).[5]

The C−H stretching region shows interesting results that help to explain the reason for stereocomplex formation. The bands at 2830 and 2855 cm^{-1} are assigned to the symmetric C−H stretching of the OCH$_3$ side groups and main chain CH$_2$ whereas the broad profile at about 2930 cm^{-1} can be assigned to the asymmetric CH$_2$ stretching. As it can be seen in Figure 5c, the location of the ν_s(CH$_3$) stretching band is essentially the same for the three samples, in spite of the fact that this group is pendant from the stereocenter present in the polyamide main chain. This constant location suggests a similar chemical environment for this side group for the three samples. Conversely, significant changes are observed for the ν_s(CH$_2$). In the amorphous P6DMT(L) sample, it is located at about 2857 cm^{-1} whereas in the crystallized P6DMT(L) sample it appears as a broad peak centered at about 2855 cm^{-1} suggesting the presence of two overlapped peaks of similar intensity. In the stereocomplex, the band shows again a relatively narrow profile, and is shifted 4 cm^{-1} to lower wavenumbers. The ν_{as}(CH$_2$) band also shows significant spectral shifts with similar features. These results strongly suggest the occurrence of different lateral

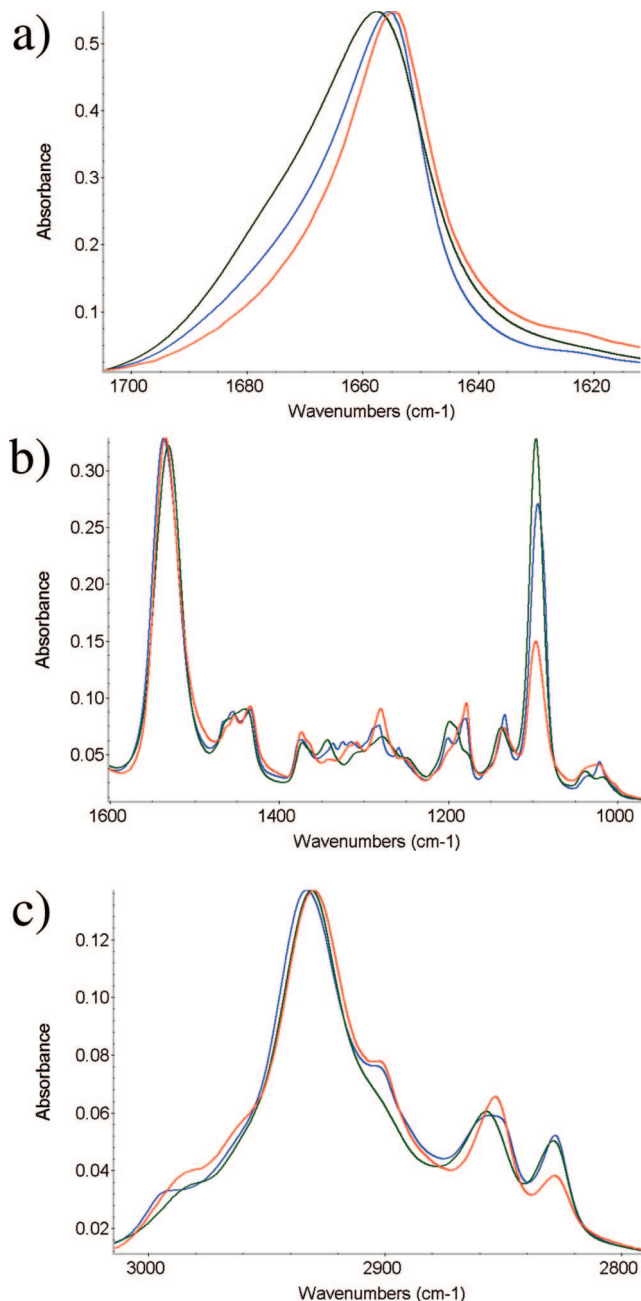**Figure 5.** Room temperature IR spectra of P6DMT(L) (green traces), P6DMT(L) crystallized at 160 °C (blue traces) and P6DMT(D+L) (red traces). Key: (a) amide I region; (b) 1000–1600 cm^{-1} region; (c) C−H stretching region.

contacts between methylene chains in P6DMT(L) and P6DMT(D+L) that could account in part for the stability of the stereocomplex.

The occurrence of different contacts between methylene groups is fully compatible with the crystal structure of P6DMT(L) and P6DMT(D+L) where hydrogen bonds are located in planes parallel to the chain direction, while methylene contacts take place in the transverse direction.[5] Whereas the packing of the OCH$_3$ side groups in the stereocomplex does not modify interchain distances in the hydrogen bonded planes, it does affect contacts in the transverse direction, where methylene−methylene interaction occurs. The favored contact between methylene groups in the stereocomplex would be due therefore to the lower steric shielding produced by the OCH$_3$ side groups in the optically compensated structure. This point will be investigated

in a near future work with the aid of molecular modeling.

The main conclusion deriving from this study is that stereocomplex formation of the stereisomeric P6DMT polyamide pair took place in solution upon aging. The stereocomplex formation entailed gelification of the mixed solution which could be visually observed. The molecular restriction caused by interlocking of the complementary enantiomeric chains was clearly manifested in the ^{1}H NMR spectra as a considerable peak broadening and it could evaluated by measuring the diffusion coefficient of the polyamide by DOSY. Evaporation to dryness of the gellified solution occurred with retention of the stereocomplex structure, as it was revealed by both DSC and infrared data. The detailed infrared analysis indicates different interchain contact between methylene units for the homopolymer and the stereocomplex.

Supporting Information Available: Text giving experimental details, a table of contact angles, and figures showing the Stejskal−Tanner plots and FTIR spectra. This material is available free of charge via the Internet at http://pubs.acs.org.

References and Notes

(1) Fox, T. G.; Garrett, B. S.; Goode, W. E.; Gratch, S.; Kincaid, J. F. *J. Am. Chem. Soc.* **1958**, *80*, 1768.

(2) (a) Baba, Y.; Kagemoto, A. *Macromolecules* **1977**, *10*, 458. (b) Grenier, D.; Prud'homme, R. E. *J. Polym. Sci., Polym. Phys.* **1984**, *22*, 577. (c) Ikada, Y.; Jamshidi, K.; Tsuji, H.; Hyon, S.-J. *Macromolecules* **1987**, *20*, 904. (d) Voyer, R.; Prud'homme, R. E. *Eur. Polym. J.* **1989**, *25*, 365. (e) Lavallee, C.; Prud'homme, R. E. *Macromolecules* **1989**, *22*, 2438. (f) Ignatova, M.; Manolova, N.; Rashkov, I.; Sepulchre, M.; Spassky, N. *Macromol. Chem. Phys.* **1995**, *196*, 2695. (g) Lim, D. W.; Park, T. G. *J. Appl. Polym. Sci.* **2000**, *75*, 1615. (h) Slivniak, R.; Langer, R.; Domb, A. J. *Macromolecules* **2005**, *38*, 5634.

(3) Domb, A. *Adv. Drug Deliv. Rev* **2003**, *55*, 549.

(4) (a) Slager, J.; Domb, A. J. *Biomaterials* **2002**, *23*, 4389. (b) Slager, J.; Domb, A. J. *Biomacromolecules* **2003**, *4*, 1316. (c) Slager, J.; Domb, A. J. *Eur. J. Pharm. Biopharm.* **2004**, *58*, 461. (d) Bishara, A.; Domb, A. J. *J. Controlled Release* **2005**, *107*, 474. (e) Tsuji, H. *Macromol. Biosci.* **2005**, *5*, 569.

(5) Iribarren, I.; Alemán, C.; Regaño, C.; Martíne de Ilarduya, A.; Bou, J. J.; Muñoz-Guerra, S. *Macromolecules* **1996**, *29*, 8413.

(6) Ruíz-Donaire, P.; Bou, J. J.; Muñoz-Guerra, S.; Rodríguez-Galán, S. *J. Appl. Polym. Sci.* **1995**, *58*, 41.

(7) Marín, R.; Alla, A.; Muñoz-Guerra, S. *Macromol. Chem. Rap. Comm.* **2006**, *27*, 1955.

(8) Bou, J. J.; Rodríguez-Galán, A.; Muñoz-Guerra, S. *Macromolecules* **1993**, *26*, 5664.

(9) Fujiwara, T.; Mukose, T.; Yamaoka, T.; Yamane, H.; Sakurai, S.; Kimura, Y. *Macromol. Biosci.* **2001**, *1*, 204.

(10) Morris, K. F.; Johnson, C. S. *J. Am. Chem. Soc.* **1992**, *114*, 3139.

(11) (a) Cabrita, E. J.; Berger, S. M. *Magn. Reson. Chem.* **2001**, *39*, S142. (b) Van Lokeren, L.; Maheut, G.; Ribot, F.; Escax, V.; Verbruggen, I.; Sanchez, C.; Martins, J. C.; Biesemans, M.; Willem, R. *Chem. Eur. J.* **2007**, *13*, 6957.

(12) (a) Zhao, T.; Beckham, H. W.; Ricks, H. L.; Bunz, U. H. F. *Polymer* **2005**, *46*, 4839. (b) Plumer, R.; Hill, D. J. T.; Whittaker, A. K. *Macromolecules* **2006**, *39*, 3878.

MA800037M